Proceedings of the 36th European Peptide Symposium
Michal Lebl (Editor)
European Peptide Society, 2022 *https://doi.org/10.17952/36EPS.2022.113*

Effect of Doubling Peptide Length on the Microscopic, Macroscopic and Biological Properties of Hydrogels

Julie Heremans[1], Lucie Chevillard[2], Morgane Mannes[1], Jessica Mangialetto[3], Jacinta F. White[4], Arthur Lamouroux[1], James Gardiner[4], Bruno Van Mele[3], Niko Van den Brande[3], Richard Hoogenboom[5], Annemieke Madder[6], Vicky Caveliers[7], Bruno Mégarbane[2], Sophie Hernot[7], Steven Ballet[1], and Charlotte Martin[1]

[1]Research Group of Organic Chemistry, Vrije Universiteit Brussel, Brussels, B-1050, Belgium; [2]INSERM, UMR-S 1144, Université de Paris, Paris, F-75006, France;[3] Physical Chemistry and Polymer Science, Vrije Universiteit Brussel, Brussels, B-1050, Belgium; [4]CSIRO Manufacturing, Bayview Avenue, Clayton, VIC 3169, Australia; [5]Supramolecular Chemistry Group, Department of Organic and Macromolecular Chemistry, Ghent University, Ghent, 9000, Belgium; [6]Organic and Biomimetic Chemistry Research Group, Ghent University, Ghent, 9000, Belgium; [7]In Vivo Cellular and Molecular Imaging, Vrije Universiteit Brussel, Brussels, 1090, Belgium

Introduction

Subcutaneous administration is often the preferred drug administration route, especially for biologicals characterized by a limited oral bioavailability. In view of chronic diseases and the associated frequent drug administrations, subcutaneous sustained drug delivery formulations were developed, of which hydrogels represent one promising subclass [1-4]. Hydrogels, classified as functional biomaterials, can be defined as a three-dimensional fiber network composed of hydrophilic polymers, which retain large amounts of water. More specifically, amphipathic peptides as low-molecular-weight building blocks render peptide-based hydrogels biocompatible, biodegradable and easy to manufacture and functionalize. Additionally, as their nanofiber network is formed through self-assembly based on non-covalent interactions (e.g. β-sheets) (Figure 1), they can be easily injected [5-7].

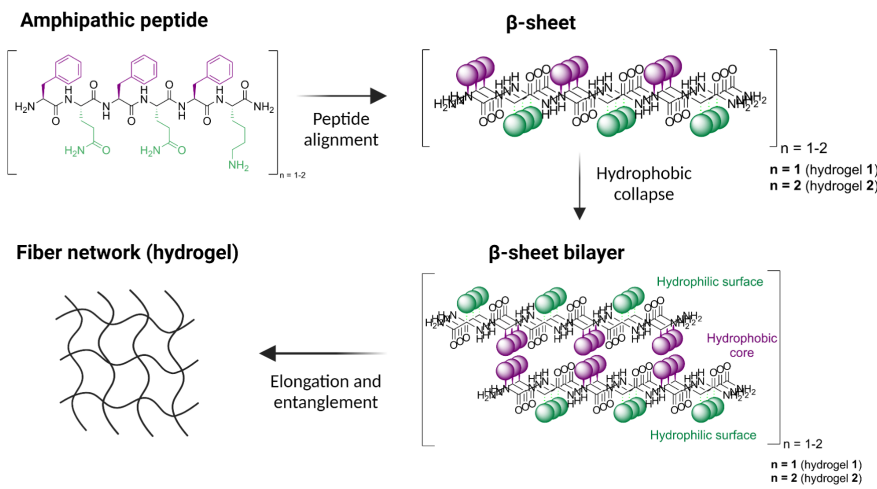

Fig. 1. Illustration of the self-assembly process of amphipathic peptide-based hydrogelators. The chemical structure of the hydrogelator is composed of alternating hydrophobic amino acids (in purple) and hydrophilic amino acids (in green).

In prior work, several hexapeptide sequences (e.g. H-FEFQFK-NH_2, H-FQFQFK-NH_2) have already demonstrated their efficacy in the delivery of therapeutically relevant molecules [8,9]. In this study, further extension of the drug release time period was aimed for by doubling the hydrogelator length, from a hexamer H-FQFQFK-NH_2 (hydrogel **1**) up to a dodecamer H-FQFQFKFQFQFK-NH_2 (hydrogel **2**), which was hypothesized to increase the amount of intermolecular interactions between the peptide chains. The effect of this doubled peptide length on the hydrogel's fiber and network morphology (microscopic), mechanical properties (macroscopic) and *in vivo* gel stability and drug release behaviour (biological properties) was evaluated.

Results and Discussion

In order to determine the influence of doubling the peptide length on the hydrogel properties, several experiments were performed using various techniques, including cryogenic and negative staining transmission electron microscopy (TEM), dynamic rheometry, *in vivo* SPECT/CT imaging and the *in vivo* hot-plate test (an antinociceptive model).

Hydrogel characterization

First of all, analyses of the two hydrogels by Fourier Transform Infrared (FT-IR) spectroscopy confirmed the presence of β-sheets as secondary structures within the entangled nanofiber networks, since a clear amide I band was visible within the 1610–1640 cm^{-1} spectral region. Subsequently, characterization of the fiber/network morphology was performed by cryogenic and negative staining TEM, which revealed that both hydrogel **1** and **2** (Figure 1) were able to form a highly intertwined nanofiber network, but there was a clear impact of the hydrogelator length on fiber morphology. While hydrogel **1** forms very long fibrils with some linear aggregation into tape like structures, hydrogel **2** forms shorter, more flexible fibrils with also some circular features in the network.

Lastly, an assessment of the hydrogel's mechanical or viscoelastic properties was possible *via* dynamic rheometry, applying a 5-step procedure after injection of the samples in between the rheometer plates. The first 2 hour time sweep (25ºC, 0.5% strain, 0.15 Hz frequency) indicated that the obtained storage moduli (G') are around 5 times higher than the corresponding loss moduli (G''), resulting in a dominant elastic or gel-like behaviour for both hydrogel systems. Remarkably, the G' of hydrogel **2** (2% w/v) (60 ± 10 Pa) is substantially lower than the G' of hydrogel **1** (2% w/v) (660 ± 160 Pa), suggesting that doubling the hydrogelator length adversely affects the gel strength (a lower rigidity was observed). Considering the cryo-TEM results, this might be explained by the shorter dodecamer fibrils and therefore lower cross-linking density of its fiber network. In step 4, an *in situ* destruction of the gels was performed (strain from 0.01% to 500%), which resulted in a phase angle (δ) increase to 90°, implying a successful viscous deformation. More importantly, a full recovery of the moduli was achieved for both gels (step 5) after destruction, with a faster recovery for hydrogel **2**, confirming the injectability of the two systems (i.e. thixotropic behaviour). Overall, as it seems challenging to relate the mechanical properties of the gels *before in vivo* injection to their observed drug release behaviour *after* injection (*vide infra*), a first experiment was performed where the mechanical properties were measured of the hydrogel **2** residue dissected from the mouse at 6h post *in vivo* injection. The resulting storage modulus (ca. 6500 Pa) was significantly higher than the pre- injection modulus (ca. 60 Pa), suggesting an influence of subcutaneous medium on the hydrogel **2** assembly and stiffness.

In vivo (SPECT/CT) imaging

After a thorough *in vitro* validation of the two hydrogels, their *in vivo* stability was investigated using non-invasive nuclear SPECT/CT imaging, which was possible by radiolabeling a fraction of the hydrogel network with radioactive isotope ^{111}Indium (using DOTA as chelator). Following injection of the ^{111}In-labelled formulations, the hydrogel volume at the injection site could be estimated by measuring the remaining radioactivity at the injection site over time. These results showed that hydrogel **2** was significantly more stable compared to hydrogel **1**, which seems to be supportive of different drug release mechanisms for the two gels (mainly diffusion-based and erosion-based, respectively).

The higher *in vivo* stability of hydrogel **2** also resulted in a more prolonged release profile of two different peptide drugs (i.e. cargoes), as observed in an *in vivo* drug release study where the ^{111}In-labelled drug was followed at the injection site via SPECT/CT imaging (Figure 2).

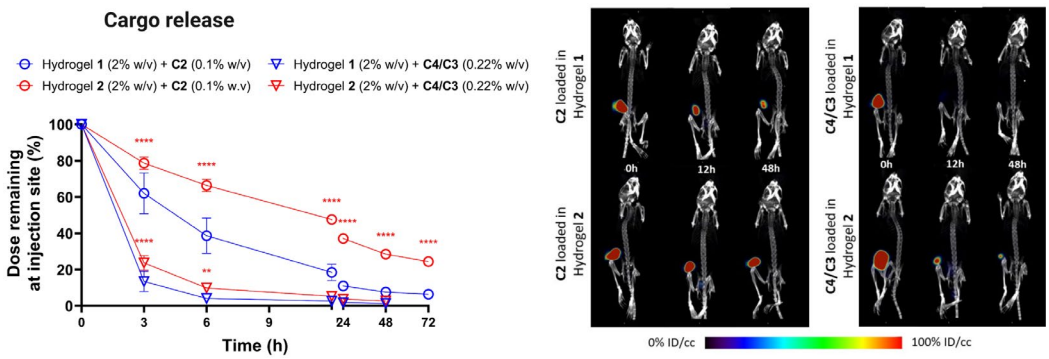

*Fig. 2. In vivo release profile (left) of cargoes **C2** (0.1% w/v) and **C4/C3** (1:1.2) (0.22% w/v) from hydrogels **1** and **2** (2% w/v gels in PBS). The radioactive signal at the injection site was quantified at different time-points post-injection, representing the remaining dose over time, presented as mean ± SD (n = 4): (**) P < 0.01, (****) P < 0.0001, hydrogel **2** vs. hydrogel **1**. Corresponding SPECT/CT images (right) were scaled to the same level (0-100 %ID/cc).*

Note that the release timeframe not only depends on the hydrogel system, but also on the cargo encapsulated. For example, the longer peptide cargo **C2** (0.1% w/v) was released from hydrogel **1** within approximately 24h, while a shorter peptide cargo, mixture **C4/C3** (1:1.2) (0.22% w/v), was released already within 6h (Figure 2). This suggests that the cargoes' physicochemical properties can influence the resulting release kinetics and are therefore important to consider.

In vivo efficacy

To evaluate the final *in vivo* efficacy of the two gels as drug delivery platform, an acute thermal nociceptive model, the hot-plate test, was performed. In specific, the mouse is restrained on a heated plate of 52 °C, at several time-points after injection of a co-formulation of the analgesic tetrapeptide **C3** (H-Dmt-DArg-Phe-Phe-NH_2, 74 µmol/kg) with hydrogel **1**, hydrogel **2** or a 0.9% NaCl solution. The results indicated that both sustained release formulations exerted prolonged analgesic effects compared to the immediate release formulation (**C3** in 0.9% NaCl solution). More importantly, hydrogel **2** caused a significant painkilling effect up to 48h post-injection, while this was up to 24h for hydrogel **1**. This longer therapeutic effect was aimed for, as it will provide a more consistent pain control and better quality of life for patients diagnosed with chronic pain.

Acknowledgements

The Research Foundation Flanders is acknowledged for funding (G054119N, 1128520N). C.M., V.C., S.H. and S.B. thank the Research Council of the VUB for the financial support through the Strategic Research Programme (SRP50). The authors thank TA Instruments for providing the Peltier Plate as well as Solvent Trap and Evaporation Blocker accessories.

References

1. Ruiz, M.E., Montoto, S.S. *ADME Processes in Pharmaceutical Sciences*, Springer, 97-133 (2018), http://dx.doi.org/10.1007/978-3-319-99593-9_6
2. Chen, W., et al. *Advanced Drug Delivery Reviews* **127**, 20-34 (2018), http://dx.doi.org/10.1016/j.addr.2018.01.016
3. Gulati, N., Gupta, H. *Recent Patents on Drug Delivery & Formulation* **5**(2), 133-145 (2011), http://dx.doi.org/10.2174/187221111795471391
4. Shi, Y., Li, L. *Expert Opinion on Drug Delivery* **2**(6), 1039-1058 (2005), http://dx.doi.org/10.1517/17425247.2.6.1039
5. Thambi, T., et al. *Journal of Controlled Release* **267**, 57-66 (2017), http://dx.doi.org/10.1016/j.jconrel.2017.08.006

6. Fichman, G., Gazit, E. *Acta biomaterialia* **10**(4), 1671-1682 (2014), https://doi.org/10.1016/j.actbio.2013.08.013
7. Martin, C., Ballet, S. *The Royal Society of Chemistry* 112-140 (2021), https://doi.org/10.1039/9781839163975-00112
8. Martin, C., et al. *Materials Today Chemistry* **3**, 49-59 (2017), http://dx.doi.org/10.1016/j.mtchem.2017.01.003
9. Martin, C., et al. *Journal of Medicinal Chemistry* **61** (21), 9784-9789 (2018), http://dx.doi.org/10.1021/acs.jmedchem.8b01282